BAREKENG: Journal of Mathematics and Its Applications
March 2025 Volume 19 Issue 1 Page 0643–0654
P-ISSN: 1978-7227 E-ISSN: 2615-3017
https://doi.org/10.30598/barekengvol19iss1pp0643-0654

3D MODELING COMPUTATION TO EVALUATE GROYNE STRUCTURE PERFORMANCE: CASE STUDY OF PASSO COASTAL AREA

Ganisa Elsina Salamena[1*], Gianita Anastasia Salamena[2], Grace Loupatty[3], Citra Fathia Palembang[4]

[1]*Department of Civil Engineering, Politeknik Negeri Ambon*
Wailela, Ambon, 97234, Indonesia

[2,3] *Department of Physics, Faculty of Science and Technology, Universitas Pattimura*
[4]*Department of Computer Science, Faculty of Science and Technology, Universitas Pattimura*
Poka, Ambon, 97234, Indonesia

*Corresponding author's e-mail: * **ganisa.salamena@polnam.ac.id***

Article History:

Received: 18th August 2024
Revised: 9th November 2024
Accepted: 9th November 2024
Published:13th January 2025

Keywords:

Coastal Sediment;
Computation Model
Delft-3D;
Groyne;
Hydrodynami.

ABSTRACT

Groyne is very important to protect the coastline with the concept of maintaining the balance of sediment transport. Groyne building in theory can work well if worked in groups or more than one. In this study, the Passo beach location was chosen because there is an existing groyne building that, if seen on Google Earth, has been damaged by the scattering of the constituent rocks. If the groyne cannot work to balance the sediment transport, it may occur that mass destruction to the infrastructure behind the groyne itself, such as regional roads, may occur. To find out the level of damage, an in-depth study needs to be carried out. In this paper, Delft-3D mathematical modeling was carried out to investigate groyne damage by looking at the performance of groyne in maintaining the balance of sediment transport in the Passo beach area. Hydrodynamic and coastal sediment modeling analyses were carried out in wet and dry season conditions. Modeling was carried out over one month with a morphology factor of 12 to obtain sediment transport for one year. In the existing dry season conditions, it shows that at the observation point, there is erosion of 2 meters, and in the wet season sediment transport is balanced. It is implied that the groyne structure must be replaced for being surpass the structure lifetime.

How to cite this article:

G. E. Salamena, G. A. Salamena, G. Loupatty and C. F. Palembang., "3D MODELING COMPUTATION TO EVALUATE GROYNE STRUCTURE PERFORMANCE: CASE STUDY OF PASSO COASTAL AREA," *BAREKENG: J. Math. & App.*, vol. 19, iss. 1, pp. 0643-0654, March, 2025.

Journal homepage: *https://ojs3.unpatti.ac.id/index.php/barekeng/*
Journal e-mail: *barekeng.math@yahoo.com; barekeng.journal@mail.unpatti.ac.id*

Research Article · Open Access

1. INTRODUCTION

One of the problems that is often faced is coastal erosion, which is a threat to people who live in coastal areas [1]. Extreme climate change also occurs with extreme coastline changes [2]. Beach erosion is caused by extreme waves and the characteristics of sandy beaches, which create a sloping topography in coastal areas [3]. Based on this, areas located in coastal areas need to be paid attention to, especially those experiencing coastal erosion [4]. Coastal erosion is a significant concern for many communities around the world, particularly in regions where urban development encroaches upon fragile shorelines. One effective solution to mitigate this issue is the construction of a groin—a structure built perpendicular to the shoreline that aims to interrupt the flow of sediment and reduce the impact of wave action. Groins serve as a critical component of coastal management strategies, helping to protect beaches from erosion while influencing sediment dynamics in their vicinity [5].

Passo Beach is located in Passo Village, Baguala District, Ambon City, around which there are residential areas and connecting roads between the city and district. One of the main problems facing Passo Beach is beach erosion. At the study location, there is a single groyne building that has been damaged and previously functioned to protect the seawall behind it, which protected the connecting road between the city and district. Several points on the sea wall also experienced erosion on the toes that were standing on sandy soil. Study before about coastal protection with groyne as the structure must be installed with a series of groins to occur the equilibrium condition.

The coastal protective structure needed a series of groynes to resist erosion and poorly distributed distribution of sediment transport, the example pictured in coastal protection at Camplong Beach, Madura, Indonesia [6]. Compared to the other study from the Comodo beach protection structure, groins effectively minimize erosion at its function [7]. Furthermore, it is necessary to conduct a study to look at the hydrodynamic conditions and sediment transport for existing conditions. This research delves into the effectiveness of groins in coastal environments. By examining a case study in Passo Beach, that aims to understand how these structures interact with natural sedimentation processes. Additionally, the study needed to explore the physics and mathematics modeling to check the groyne condition through a comprehensive analysis of current literature and field data; this study seeks to provide insights into the best practices for hydrodynamic computation, contributing to more coastal management research.

The hydrodynamic computation is accommodated by Delft3D software. To begin with, define the study area to collect the data on water levels, currents, and sediment transport characteristics from the Ambon-Baguala Bay coastal area. Moreover, the model domain was created to capture the necessary detail around the groyne structure. Also, set up the boundary conditions. Then, represent the groyne as a structure in the model. Assign appropriate roughness values and other hydraulic properties to simulate the effect of the groyne on flow patterns. Configure sediment transport parameters to model to display how the groyne influences sediment deposition and erosion [8]. At last, compare the model results with observed data.

The result is to conduct a visualization of how currents flow around structures. Mapping the sediment accumulation and erosion areas is crucial for understanding long-term coastal changes. Collect the quantitative data on sediment transport rates and directions, helping to predict changes in shoreline morphology. Analyzed wave transformation as they approach the coast, including refraction and diffraction effects. Identification of areas where waves break and their impact on coastal erosion and sediment dynamics. Furthermore, to evaluate how the groyne structure effectively influences the coastal sediment transport process on Passo Beach.

2. RESEARCH METHODS

2.1 Hindcasting

Hindcasting conducts the wind data correction, analysis of wave height based on wind and wave generation (fetch) area. Based on Join North Sea Wave Project Spectrum (JONSWAP) model that used in oceanography and marine science to describe the wave energy distribution in the surface of ocean. Originally developed to describe waves in the North Sea, this model has been widely adopted and developed for various water case effectively until now [9]. JONSWAP hindcasting method [10]:

a. To check if the wave is fully developed or not, use the formulation:

$$\frac{g \cdot t}{U_A} = 68{,}8 \left(\frac{g \cdot F}{{U_A}^2}\right)^{2/3} \quad (1)$$

g : gravitational acceleration

t : wind duration

U_A : wind velocity after shear correction

F : fetch

Check if:

$$\text{Fully Developed: } \frac{gt}{U_A} > 7.15 \times 10^4 \quad (2)$$

$$\text{Not Fully Developed: } \frac{gt}{U_A} \leq 7.15 \times 10^4 \quad (3)$$

b. Time of concentration (t_c) formulation:

$$\text{Fully Developed: } t_c = 7.15 \times 10^4 \left(\frac{U_A}{g}\right) \quad (4)$$

$$\text{Not Fully Developed: } t_c = 68.8 \left(\frac{g \cdot F}{{U_A}^2}\right)^{2/3} \left(\frac{U_A}{g}\right) \quad (5)$$

c. Wave Height (H_{m0}) and Period (T_P)

Fully developed:

If $t \geq t_c$ (fetch limited),

$$H_{m0} = 0.2433 \left(\frac{{U_A}^2}{g}\right) \quad (6)$$

$$T_P = 8.134 \left(\frac{U_A}{g}\right) \quad (7)$$

If $t < t_c$ (duration limited),

$$H_{m0} = 0.0016 \left(\frac{{U_A}^2}{g}\right) \left(\frac{g \cdot F_{min}}{{U_A}^2}()^{1/2}\right) \quad (8)$$

$$T_P = 0.2587 \left(\frac{U_A}{g}\right) \left(\frac{g \cdot F_{min}}{{U_A}^2}()^{1/3}\right) \quad (9)$$

with:

$$F \left(\frac{g \cdot t}{68.8 \cdot U_A}\right)^{3/2} \frac{{U_A}^2}{g}_{min} \quad (10)$$

F_{min}: Fetch Minimum

Non-Fully Developed:

If $t \geq t_c$ (fetch limited),

$$H_{m0} = 0.0016 \left(\frac{{U_A}^2}{g}\right) \left(\frac{g \cdot F}{{U_A}^2}\right)^{1/2} \quad (11)$$

$$T_P = 0.2857 \left(\frac{U_A}{g}\right) \left(\frac{g \cdot F}{{U_A}^2}\right)^{1/3} \quad (12)$$

If $t < t_c$ (duration limited),

$$H_{m0} = 0.0016 \left(\frac{{U_A}^2}{g}\right) \left(\frac{g \cdot F_{min}}{{U_A}^2}()^{1/2}\right) \quad (13)$$

$$T_P = 0.2587 \left(\frac{U_A}{g}\right) \left(\frac{g \cdot F_{min}}{{U_A}^2}()^{1/3}\right) \quad (14)$$

The result of the JONSWAP method will draw a wave-rose diagram [11]. The aim of processing the wind data and fetching it is to identify the dominant wave that contributes to sediment processes. The dominant wave is different from an extreme wave. The dominant wave is defined as the wave that occurred repeatedly or had the majority of intensity in the time being. Meanwhile, the extreme wave is defined as the highest wave that occurs in a period.

2.2 Wave Computation

Delft University of Technology developed a model called SWAN. The SWAN model is used to study coastal and nearshore modeling [12]. Therefore, Deltares integrated the SWAN model into a series of Delft3D models [13]. Under the public domain, the SWAN model has been released. In the development of SWAN regarding the wave spectrum, the mathematical equation for the physics of spectral action balance is described for Cartesian coordinates as:

$$\frac{\partial}{\partial t}N + \frac{\partial}{\partial x}C_x N + \frac{\partial}{\partial y}C_y N + \frac{\partial}{\partial \sigma}C_\sigma N + \frac{\partial}{\partial \theta}C_\theta N = \frac{S}{\sigma} \quad (15)$$

with density of spectrum (N)

The first term in the left-hand side of this equation represents the local rate of change of action density in time. The second and third terms represent geographical space propagation (with velocity of propagation C_x and C_y in x and y space, respectively). The fourth term represents the relative frequency shifting due to variations in depths and currents (with propagation velocity $\partial\sigma$ in σ-space). The fifth term represents depth-induced and refraction of current induces (with velocity of propagation C_θ in θ-space) [14].

2.3 Flow Computation

Navier-Stokes equations for incompressible fluids, under shallow water and Boussinesq assumptions applied to Delft3D Flow [15]. Neglecting vertical acceleration in the vertical momentum equation then results in the hydrostatic pressure equation. Vertical velocity is calculated from the continuity equation in the 3D model [16]. The Reynolds-averaged Navier-Stokes equation may be written as:

$$\frac{\partial u_i}{\partial t} + u_i\frac{\partial u_j}{\partial c_i} + \frac{1}{\rho_0}\frac{\partial u}{\partial x_i} + \frac{1}{\rho_0}\frac{\partial \tau_{ij}}{\partial x_i} + \varepsilon_{ijk}2\Omega_j u_k = \frac{\rho}{\rho_0}g\delta_i \quad (16)$$

With the Kronecker delta ∂_{ij}, the symbol of permutation ε_{ijk}, the symbol of planetary vorticity Ω_j and are the symbol of turbulent stresses τ_{ij} [17].

2.4 Sediment Transport Concept

In an open boundaries, the user can specify the bed load delivery rates or the bed development rates [18]. In the latter case the bedload transport rates are known from the model input, whereas in the former case the effective bedload transport rates at the boundary could be derived from the mass balance at the open boundary point. At the U and V points **Figure 1** as this ensures that the bed will remain stable [19]. By adding the components of bed load transport at the water level points on either side of the velocity point and taking the upwind direction relative to the resulting net transport direction can determine the upwind direction, for each active velocity point [20].

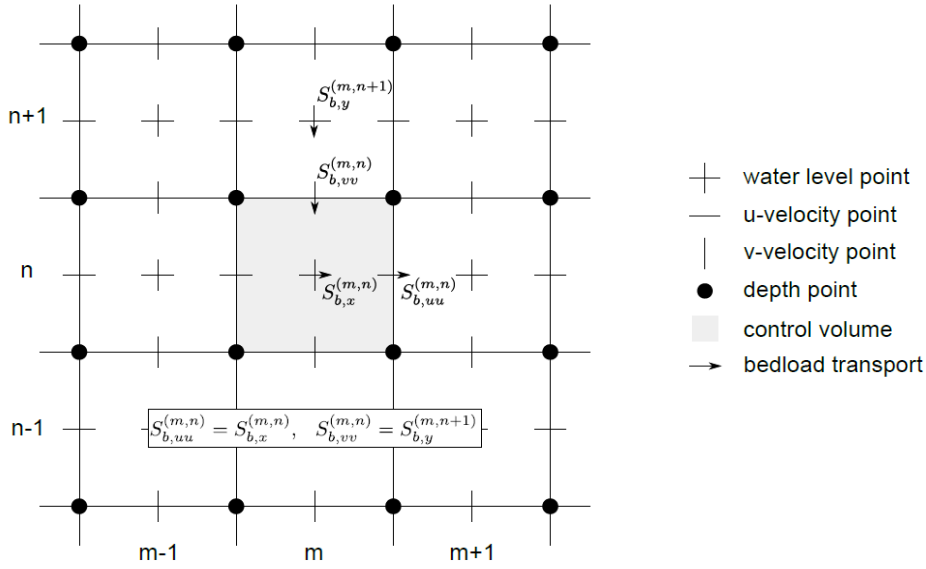

Figure 1. Delft3D Flow Bedload Transport Components at Velocity Points
***Source**: delft3D Flow Manual*

Component of the bed load component $S_{b,uu}^{(m,n)}$ is set equal to $S_{b,x}^{(m,n)}$ and the component $S_{b,vv}^{(m,n)}$ is set to equal $S_{b,y}^{(m,n+1)}$.

3. RESULTS AND DISCUSSION

3.1 Existing Area

The hindcasting calculation setting is in the Ambon-Baguala Bay area at the point of damage **Figure 2**. The study location is at the deepest point of the bay so the modeling process is carried out not only at the study location but also throughout Ambon Baguala Bay.

Figure 2. Passo Beach Existing Groyne Condition Plotting
***Source:** Google Earth*

3.2 Wave Rose-Hindcasting

JONSWAP hindcasting uses the 10 years of wind velocity historical data collected from the Indonesian Agency for Meteorological, Climatological, and Geophysics (BMKG), a fetch line that draws from the

research area to the deep-sea area, and the results are presented as a wave-rose diagram in **Figure 3** and **Figure 4** for each season, using WRplot Program 8.0.2 version

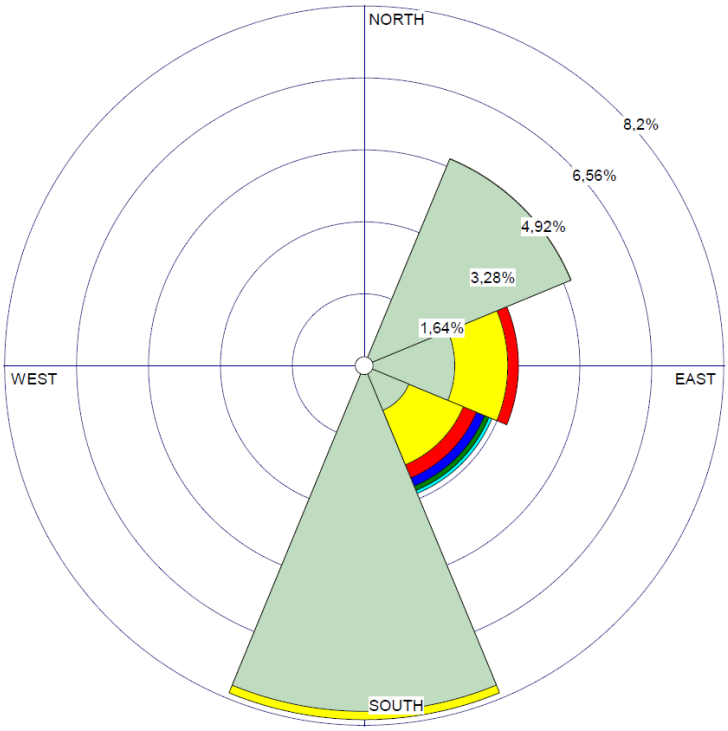

Figure 3. Wave-Rose for Dried Season
Source: *WRplot Program 8.0.2 Version*

Wave-rose for dried season after fetch elimination at **Figure 3**, implied that the dominant wave occur from south but it happen to be non-extreme value. Furthermore, waves that occurred from the southeast indicated the extreme value. The modeling computation uses the wave height from the south because the dominant wave is a major factor in coastal flow conditions that occur in the sediment transport process.

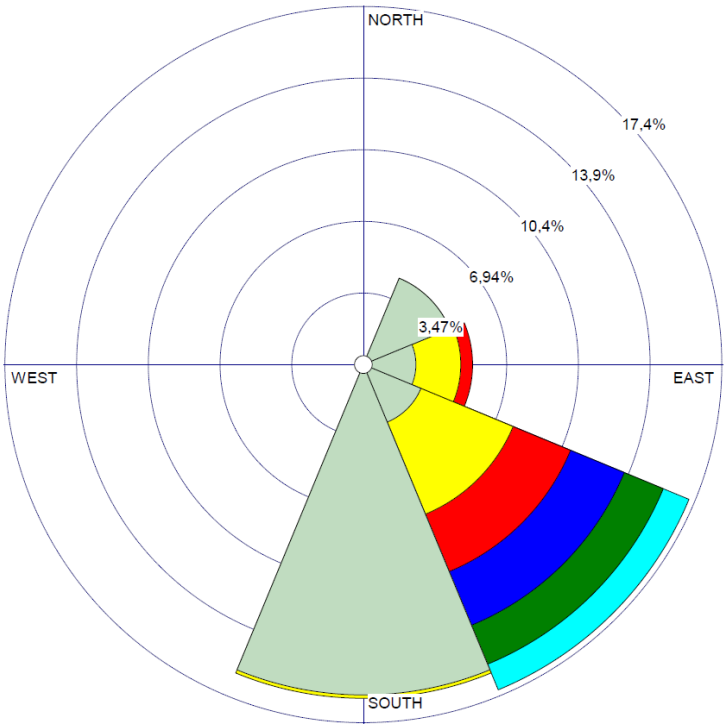

Figure 4. Wave-Rose for Wetted Season
Source: *WRplot Program 8.0.2 Version*

The wetted season wave-rose provides information about the dominant and the extreme wave height from the southeast. It is clear to use the values from the south-east to model the flow computation. With the result of wave hindcasting, recapitulation of wave significant height (H_s) and its period (T_s) show:

Wetted season; H_s = 0,4 m; T_s = 3.1 s (from South)

Dried season; H_s = 1,1 m; T_s = 5.5 s (from Southeast)

3.3 Delft 3D Model Set Up

The grid used in the simulation is in the form of a Coordinate Spherical. Grid creation uses Delft3D-RGFGRID. The grid used is curvilinear by utilizing nesting or joining the main grid with a secondary grid at the study location whose purpose is to shorten the time of modeling. The size of the grid at the study location is 5x5 meters. The time frame setting consists of a simulation time reference and a time step to conduct simulations. Used time: 15 days on time tidal measurement with a timestep of 0.5 minutes.

To ensure that the model from Delft 3D software works accurately, the deft3D open boundary tides data from the Delftdashboard is calibrated to the real-time tides observation data in **Figure 5** and **Figure 6**.

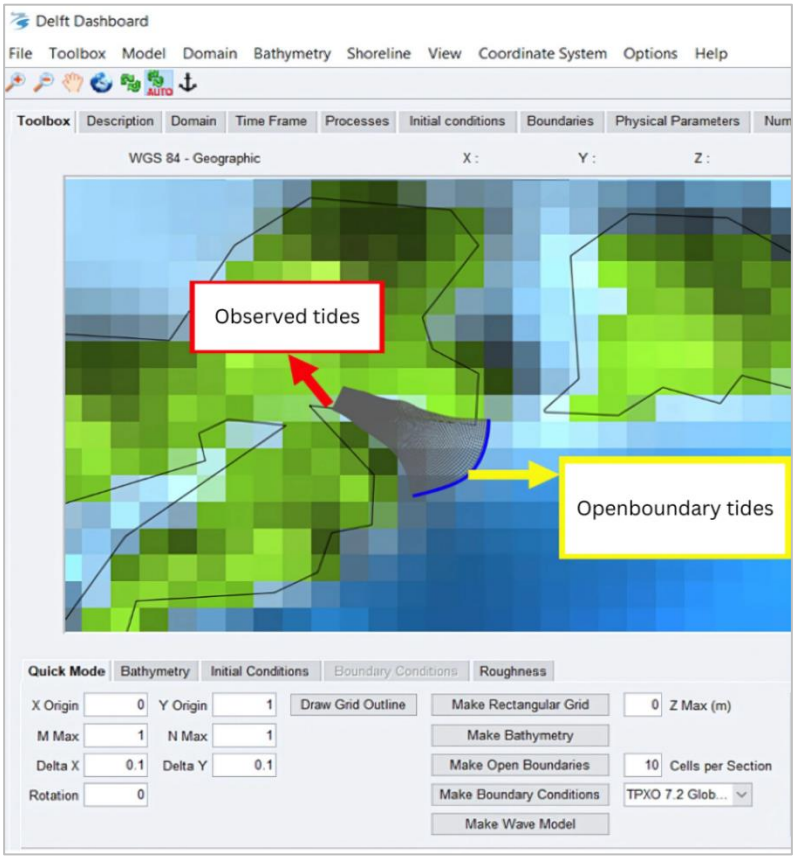

Figure 5. Delft Dashboard Tides Location and Observed Tides Location
Source: *DelftDashboard Delft 3D 4.03.01 Version*

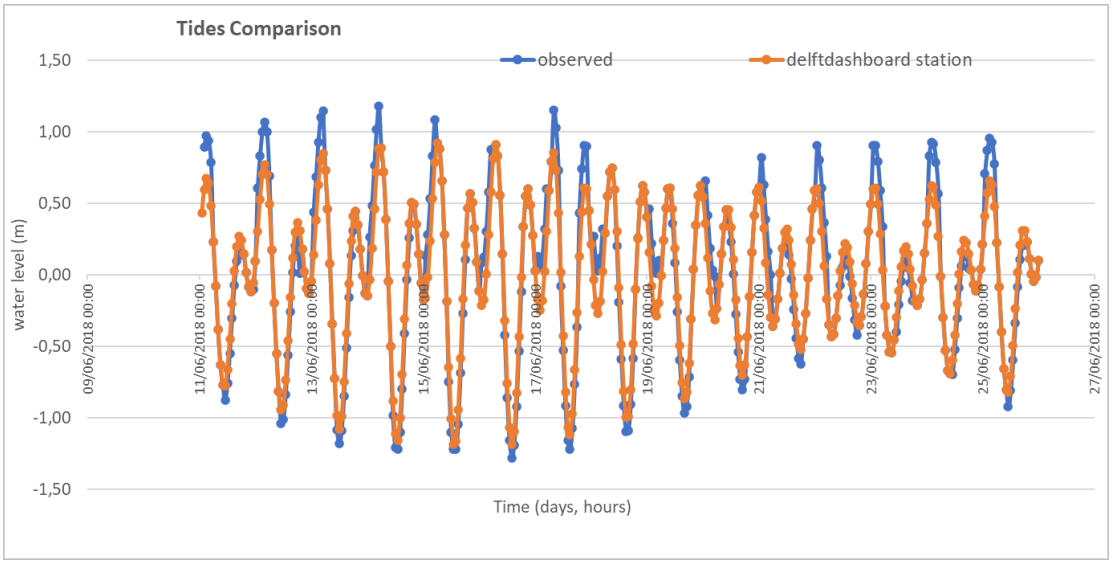

Figure 6. Tides Comparison

The results of the model validation with correlation show a 97% data match with an error rate of 8% in the Root Mean Square Error method. So that modeling can be carried out using Delft3D. The modelling process then has two scenarios. At the beginning, the simulation performs the wetted season month (March to October), then followed by the dried season simulation (October to March) to identify the effect of each season on the research study sediment transport process.

3.4 Wetted Season Modeling

Delft 3D Flow was used to simulate tides and sediments, and Delft 3D Wave was used for wave propagation analysis. The input uses the result from hindcasting and the bathymetry for the Ambon-Baguala Bay area that was collected from surveying analyses. The soil from the sediment sample had been processed in the laboratory as the result of soil properties in addition to Delft 3D processing.

The results of the Delft3D-Wave modeling for the existing wetted season depict wave propagation from the southeast direction, and in the propagation pattern, there is a shallowing pattern at the coral reef location in location A in **Figure 7**, but because the elevation of the coral reef peak is -5 meters, overtopping occurs with a reduction in wave energy, and in the area after the coral reef, there is a decrease in the sea bed elevation of 20 meters, causing waves due to the influence of the wind to form.

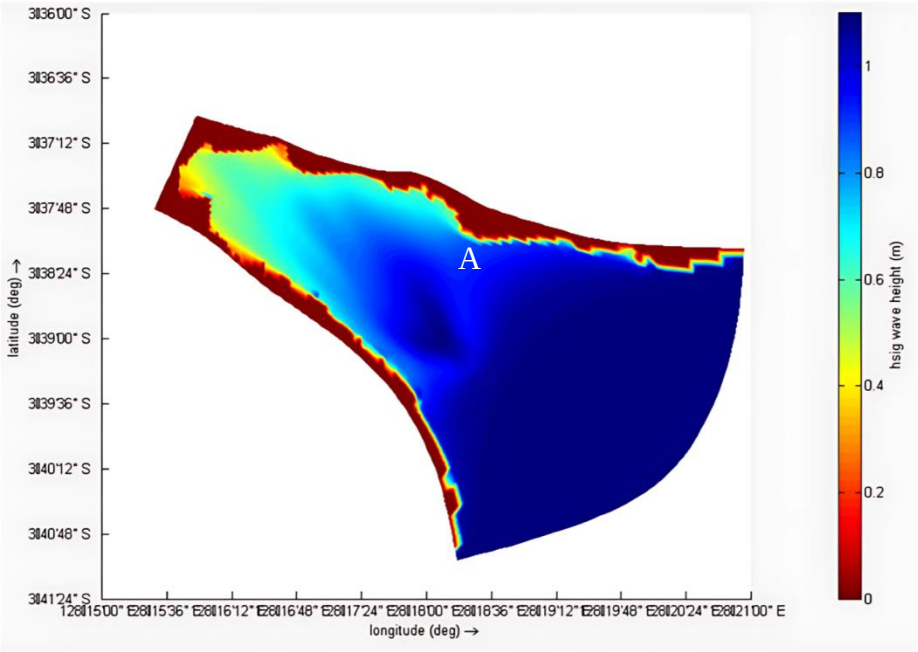

Figure 7. Wave Propagation Analysis for Wetted Season

Source: *Delft3D 4.03.01 Version*

The wave propagation in that picture with spectral color shows the smoothing shoaling process in the study area, and the wave refraction shows as well. This result is also carried in the Delft3D-flow process to support the sediment modeling that shows in **Figure 8**.

Besides the Delft-Wave result, to conduct the Delft-3D Flow model required the additional data, such as soil properties data. The soil characterized as sandy (non-cohesive) that measured:

Specific density = 2650 Kg/m^3
Dry bed density = 1600
D50 = 540 µm
With layer thickness = 2 m

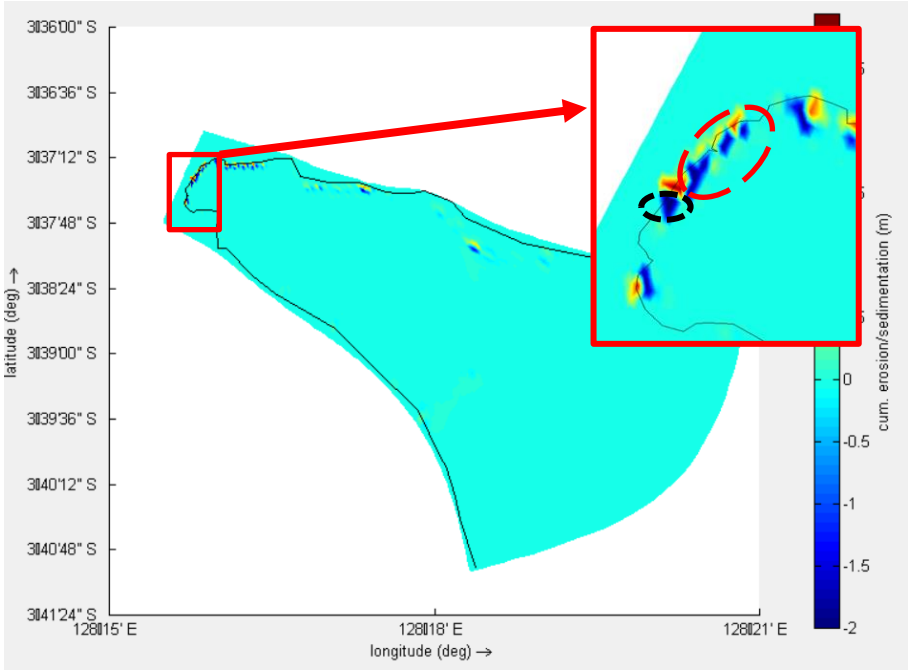

Figure 8. Flow-Sediment Simulation for Wet Season Modeling with delft3D
Source: *Delft3D 4.03.01 Version*

Describe in **Figure 8** how longshore occurs due to oblique waves, because at the front of the bay there is an obstacle in the form of a submerged coral reef, making the current direction tend to be straight on the right side of the bay, and towards the perpendicular to the beach (view area), the current pattern turns to the southwest. due to the obstructive influence of land jutting into the sea.

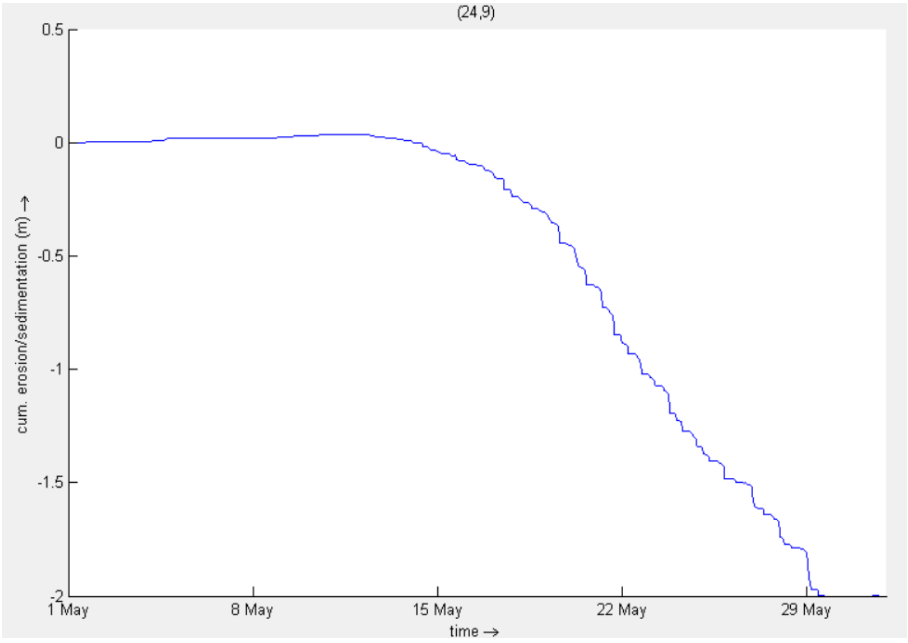

Figure 9. The Accumulation of Sediment Transport at the Existing Groyne Area (Wetted Season)
***Source**: Delft3D 4.03.01 Version*

The results of the sedimentation modeling for 1 year (accumulated from a month of modeling with a morphology factor of 12 to repeat the tides phenomenon at the Passo Beach area) of the existing wet season show that the area to the southwest (from a review of the location of the damaged groyne) experienced erosion of 2 meters (**Figure 9**). It is proffered that the groyne malfunctioning as the coastal area protection building.

3.5 Dried Season Modeling

Same as the dry season model, use the input from the JONSWAP hindcasting method result, but fit the seasonal data required. For this model, use the dried season result.

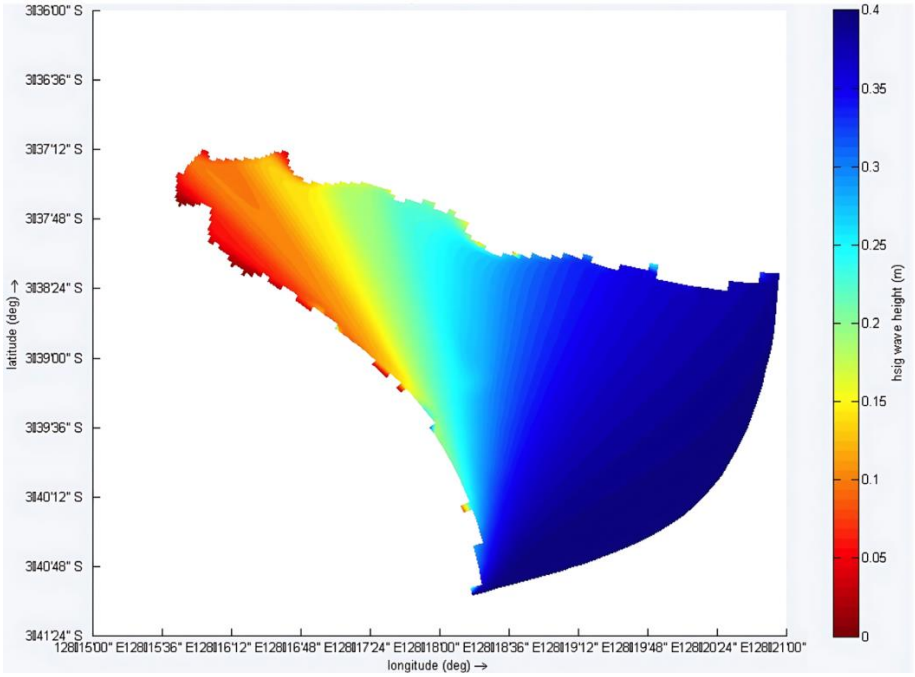

Figure 10. Wave Propagation Analysis for Dried Season
***Source:** Delft3D 4.03.01 Version*

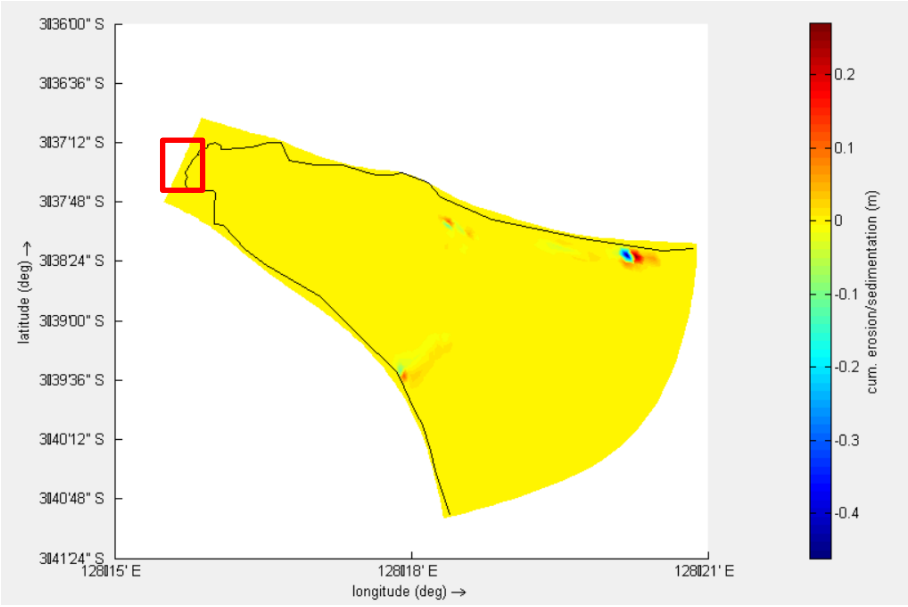

Figure 11. Flow-Sediment Simulation for Dried Season (Red Boundary is the Passo Coastal Area)
***Source**: Delft3D 4.03.01 Version*

The direction of the wave coming from the south makes the angle of the wave tend to be oblique at the study location. The propagation process involves many obstacles, and refraction and diffraction processes occur, resulting in the wave energy being reduced when it arrives at the study location (**Figure 11**). The wave spectral display of the refraction process is very smooth. Different from the wetted season that had an impact from the coral reef in the beginning of the Tial coastal area, the dried season turned the wave breaking early from the beginning of the wave propagation. The result from wave modeling is used as the base data to run the flow modeling program and is shown as **Figure 11**. The results of dry season sediment modeling for existing conditions show that the study location (red boundary) did not experience erosion or sedimentation. Sediment modeling indicates stability in the study area during the dry season. This could suggest effective natural processes or existing land management practices that prevent erosion and sedimentation.

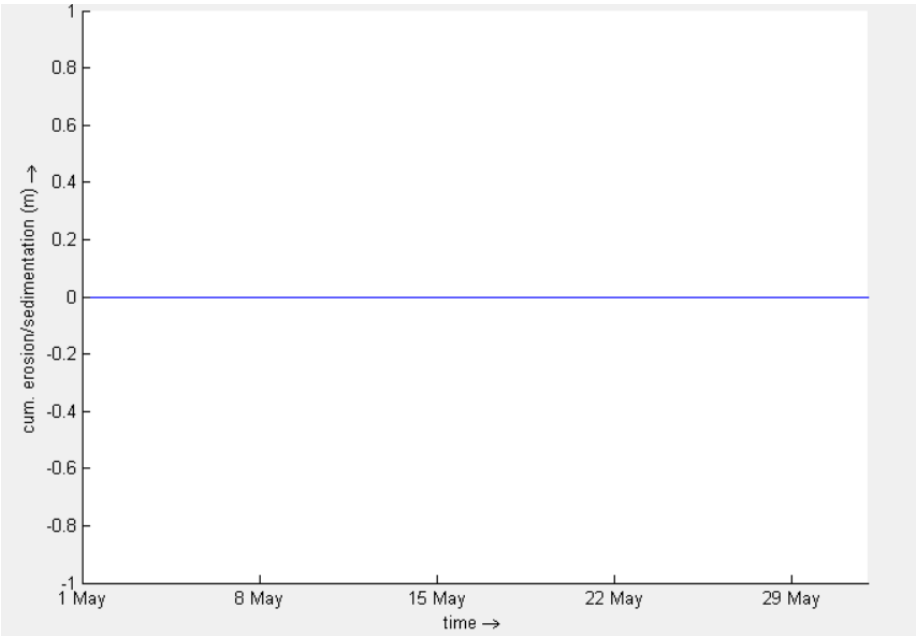

Figure 12. The Accumulation of Sediment Transport at the Existing Groyne Area (Wetted Season)
***Source**: Delft3D 4.03.01 version*

The accumulation of sediment transport is also steady at zero in **Figure 12**, because the direction of the wave comes from the south, and the wave height is not as big as in the dry season, and when it arrives at the study location, it experiences a large reduction in energy. The point of view of the dried season opposed the wetter season; the equilibrium state of sediment transport eventuated in the research location.

4. CONCLUSIONS

In the wet season, a sediment transport process occurs from the northeast to the southwest along the coastline, resulting in erosion of 2 meters during one year in the review area, especially in the southwest direction of the damaged groyne location. In dry season, sediment transport along the Passo coast tends to be balanced so that the cumulative value is zero for one year. This result implied that the Passo coastal area requires the replacement of existing groyne to retain the existing shoreline and also to protect the property behind.

REFERENCE

[1] S. A. Suleman and S. Bur, "MITIGASI BENCANA ABRASI DAN SEDIMENTASI PANTAI PADA DI PESISIR PANTAI KABUPATEN PANGKEP," *Ris. Sains dan Teknol. Kelaut.*, 2023, doi: 10.62012/sensistek.v6i1.24250.

[2] S. A. Antarissubhi. H, Serang Rudi, Leda Jeremias, Salamena Ganisa Elsina, Pagoray Gebion Lysje, Gusty Sri, Rachman Ranno Marlany, *Krisis Iklim Global di Indonesia (Dampak dan Tantangan)*. 2023. [Online]. Available: https://books.google.co.id/books?hl=id&lr=&id=xsjcEAAAQBAJ&oi=fnd&pg=PP1&ots=nIAoTe_upJ&sig=MgAfoC6vQ0WDLZDnQ-tqWXzA81o&redir_esc=y#v=onepage&q&f=false

[3] N. Khakhim, F. Yasidi, D. Mardiatno, and A. Kurniawan, "Modeling Lasolo Watershed Sedimentation and Mangrove Root Growth at the Lasolo Coast in North Konawe, Indonesia," *J. Environ. Manag. Tour.*, vol. 14, no. 1, 2023, doi: 10.14505/jemt.v14.1(65).10.

[4] A. Isdianto, I. M. Asyari, M. F. Haykal, F. Adibah, M. J. Irsyad, and S. Supriyadi, "ANALISIS PERUBAHAN GARIS PANTAI DALAM MENDUKUNG KETAHANAN EKOSISTEM PESISIR," *Jukung (Jurnal Tek. Lingkungan)*, vol. 6, no. 2, 2020, doi: 10.20527/jukung.v6i2.9260.

[5] Dalrino, R. Herdianto, and D. B. Silitonga, "Study of groin structures effectiveness for against abrasion in Padang Beach," in *IOP Conference Series: Earth and Environmental Science*, IOP Publishing Ltd, Apr. 2021. doi: 10.1088/1755-1315/708/1/012035.

[6] Y. N. Purnawanti, L. D. Ayunda, and A. R. Santoso, "Studi Perencanaan Revetment dan Groin Sebagai Upaya Penanganan Erosi Pantai Camplong di Kabupaten Sampang Madura," *J. Tek. Transp.*, vol. 1, no. 1, p. 70, Apr. 2020, doi: 10.54324/jtt.v1i1.431.

[7] W. Tribhaskoro, S. Widada, and W. Atmodjo, "Sedimentasi di Sekitar Bangunan Groin di Pantai Komodo Kota Tegal," *Indones. J. Oceanogr.*, vol. 4, no. 3, pp. 01–12, Aug. 2022, doi: 10.14710/ijoce.v4i3.13261.

[8] L. Brakenhoff, R. Schrijvershof, J. van der Werf, B. Grasmeijer, G. Ruessink, and M. van der Vegt, "From ripples to large-scale sand transport: The effects of bedform-related roughness on hydrodynamics and sediment transport patterns in delft3d," *J. Mar. Sci. Eng.*, vol. 8, no. 11, pp. 1–25, Nov. 2020, doi: 10.3390/jmse8110892.

[9] W. L. Dhanistha, Suntoyo, D. M. Rosyid, and R. Akbar, "Design of wave spectrum in the Java Sea," in *IOP Conference Series: Earth and Environmental Science*, 2024. doi: 10.1088/1755-1315/1298/1/012028.

[10] K. Kuswartomo, B. N. Sulistiya, I. Isnugroho, and A. K. Fatchan, "Prediksi Tinggi Gelombang Berdasarkan CERC (SPM 1984) di Pantai Baru, Bantul, Daerah Istimewa Yogyakarta," *Din. Tek. Sipil Maj. Ilm. Tek. Sipil*, vol. 14, no. 1, 2021, doi: 10.23917/dts.v14i1.15271.

[11] A. Rahmatullah, C. Umam, W. S. Pranowo, J. Setiyadi, and A. Agustinus, "Karakteristik Angin dan Gelombang di Perairan Selatan Pulau Biak untuk Perencanaan Awal Pembangunan Dermaga Lanal," *J. Chart Datum*, vol. 8, no. 2, 2022, doi: 10.37875/chartdatum.v8i2.143.

[12] F. Suciaty and A. Setiawan, "SEDIMENTASI DI PANTAI SANTOLO WILAYAH PESISIR SELATAN JAWA BARAT DAN MODEL PENANGGULANGANNYA," *J. Kelaut. Nas.*, vol. 16, no. 1, 2021, doi: 10.15578/jkn.v16i1.9778.

[13] J. Wang, A. Chu, Z. Dai, and J. Nienhuis, "Delft3D model-based estuarine suspended sediment budget with morphodynamic changes of the channel-shoal complex in a mega fluvial-tidal delta," *Eng. Appl. Comput. Fluid Mech.*, vol. 18, no. 1, 2024, doi: 10.1080/19942060.2023.2300763.

[14] J. G. Rueda-Bayona, A. F. Osorio, and A. Guzmán, "Set-up and input dataset files of the Delft3d model for hydrodynamic modelling considering wind, waves, tides and currents through multidomain grids," *Data Br.*, vol. 28, 2020, doi: 10.1016/j.dib.2019.104921.

[15] Deltares, "DELFT3D-FLOW: 3D/2D modelling suite for integral water solutions. Simulation of multi-dimensional hydrodynamic flows and transport phenomena, including sediments. User Manual," 2020.

[16] L. Brakenhoff, R. Schrijvershof, J. van der Werf, B. Grasmeijer, G. Ruessink, and M. van der Vegt, "From ripples to large-scale sand transport: The effects of bedform-related roughness on hydrodynamics and sediment transport patterns in delft3d," *J. Mar. Sci. Eng.*, vol. 8, no. 11, 2020, doi: 10.3390/jmse8110892.

[17] Deltares, "User Manual : Delft3D - Flow," *User Man.*, vol. Version :, 2020.

[18] A. Chrysanti *et al.*, "Prediction of shoreline change using a numerical model: case of the Kulon Progo Coast, Central Java," *MATEC Web Conf.*, vol. 270, 2019, doi: 10.1051/matecconf/201927004023.

[19] T. P. Huff, R. A. Feagin, and J. Figlus, "Delft3D as a Tool for Living Shoreline Design Selection by Coastal Managers," *Front. Built Environ.*, vol. 8, 2022, doi: 10.3389/fbuil.2022.926662.

[20] P. Kumar and N. Leonardi, "Coastal forecast through coupling of Artificial Intelligence and hydro-morphodynamical modelling," *Coast. Eng. J.*, vol. 65, no. 3, 2023, doi: 10.1080/21664250.2023.2233724.